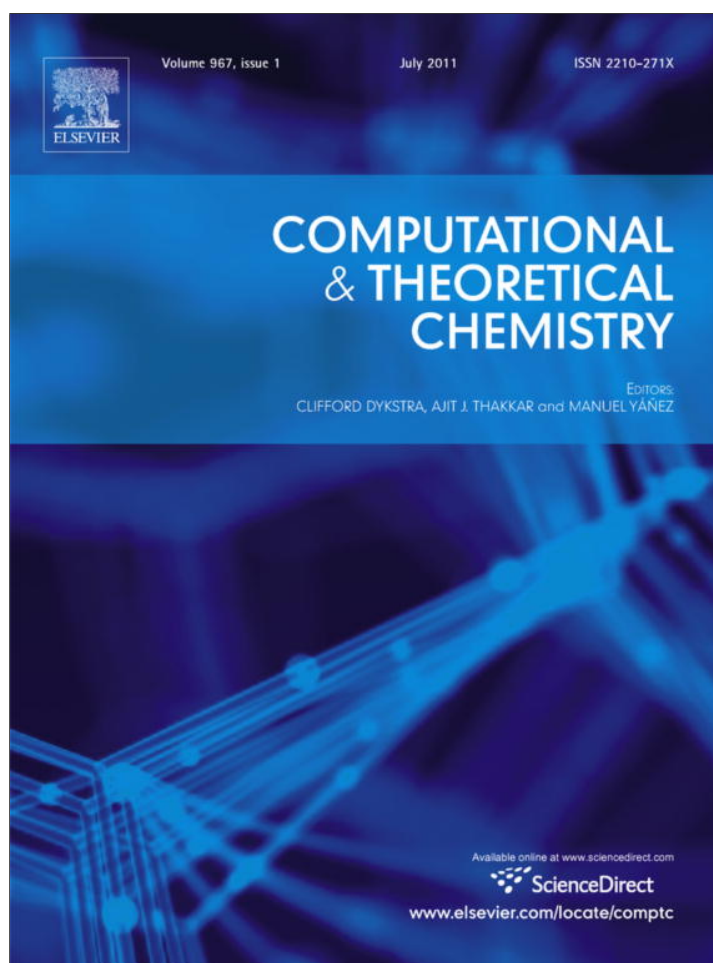


Provided for non-commercial research and education use.
Not for reproduction, distribution or commercial use.



This article appeared in a journal published by Elsevier. The attached copy is furnished to the author for internal non-commercial research and education use, including for instruction at the authors institution and sharing with colleagues.

Other uses, including reproduction and distribution, or selling or licensing copies, or posting to personal, institutional or third party websites are prohibited.

In most cases authors are permitted to post their version of the article (e.g. in Word or Tex form) to their personal website or institutional repository. Authors requiring further information regarding Elsevier's archiving and manuscript policies are encouraged to visit:

<http://www.elsevier.com/copyright>



Contents lists available at ScienceDirect

Computational and Theoretical Chemistry

journal homepage: www.elsevier.com/locate/comptc

Does structural variation in the aziridinium ion facilitate alkylation?

Pradip Kr. Bhattacharyya^{a,*}, Rahul Kar^b^a Department of Chemistry, Arya Vidyapeeth College, Guwahati, Assam, India^b Department of Chemistry, Dibrugarh University, Dibrugarh, Assam, India

ARTICLE INFO

Article history:

Received 31 October 2010

Received in revised form 13 March 2011

Accepted 13 March 2011

Available online 21 March 2011

Keywords:

Aziridinium ion

Alkylation

DFT

Reactivity descriptors

ABSTRACT

The reactivity and stability of the tricyclic aziridinium ion intermediate of the mustard drug molecule varies with the $\angle\text{NCC}$ bond angle (from 60° to 150°) of the tricyclic ring. As $\angle\text{NCC}$ bond angle increases, the tricyclic ring of the aziridinium ion opens up which leads to variation in its reactivity. We have observed shifting of the reactive center (i.e., the LUMO) of the drug intermediate with variation in the $\angle\text{NCC}$ bond angle in gas phase as well as in aqueous phase. It was also observed that the drug intermediate must undergo some structural changes before alkylating DNA. In addition, the maximum hardness principle and minimum electrophilicity principles were analyzed.

© 2011 Elsevier B.V. All rights reserved.

1. Introduction

It is a well known that the structure of an intermediate species plays important role in chemical as well as biochemical reactions. During the course of a reaction, intermediates undergo some structural changes [1]. Recently, it was shown that the chemical reactivity of a drug intermediate in the body fluid can be followed with the density based global and local reactivity descriptors [2]. However, in an important contribution from Pal et al. it was demonstrated that the hardness changes with the structure of water molecule [3]. They made a critical study on the validity of maximum hardness principle using the highly correlated wave function method by considering the symmetric and asymmetric variations around the equilibrium [3].

The nitrogen mustards represent the earliest and perhaps the most extensively studied DNA inter-strand cross-linking agents. They have been using in cancer chemotherapy for more than five decades [4–6]. Even today, mustard is one of the heavily employed clinical anticancer agents [7]. Although these bisalkylating agents have been studied and clinically exploited for several decades, they still provide an area of extremely intense and progressive investigation. During alkylation of DNA, these drug molecules form a very reactive aziridinium ion intermediate which reacts with different nucleophilic centers in biomolecules [8,9]. Calabresi et al. and Borch et al. independently suggested that the alkylation of DNA bases by these drug molecules is the favored mechanism [10]. Moreover, the alkylation occurs preferentially at the endocyclic nitrogen and

exocyclic oxygen atoms of DNA bases [11,12]. Each of the chloroethyl side chains of the nitrogen mustards spontaneously cyclizes to form aziridinium ion that finally binds to DNA, resulting a mono-adduct. This mono-adduct can react with a second DNA strand to afford a cross-linked product. For detail understanding, this one may refer to Pullman et al. [13]. In an important work, the quantum chemical calculations validate that out of different nucleophilic sites in DNA bases, N-7 position of guanine is the most nucleophilic and was shown to be a highly preferred site over others for alkylation [14,15]. In addition, the formation of the mono-adduct as well as the cross-linked product during alkylation (by inter- and intra-strand cross-linking) is well established and the mono-adduct is found to be the major product [16]. Depending on the relative stability of the aziridinium ion intermediate, the overall reaction may follow S_N1 or S_N2 pathways [17,18]. Thus, the reactivity of the aziridinium ion intermediate plays an important role during the alkylation process.

The reactivity descriptors, defined within the framework of density functional theory, are chemical potential, global hardness, softness, electrophilicity index etc. [19]. These descriptors have been tested and studied in the literature by several research groups and are found to be very useful in rationalizing the reactivity patterns of the molecular systems [20–22]. In general, the descriptors are classified as global reactivity descriptors or local reactivity descriptors. The global reactivity descriptors describe about the overall stability of the system. On the other hand, the local counterpart describes the site reactivity and selectivity. Since most of these descriptors are the derivatives of energy and electron density variables, it is expected that they will provide the information of reactivity in the molecular systems [24]. Geerlings et al. and Chattaraj et al. have recently reviewed the theoretical basis for these

* Corresponding author.

E-mail addresses: prdpbhatta@yahoo.com (P.Kr. Bhattacharyya), rahul.kar-dib@gmail.com (R. Kar).

descriptors and their applications in various molecular system [23]. Recently, the exact conditions for which the electrophilicity index experiences an extremum along an arbitrary reaction path were studied [27].

During the alkylation process, the aziridinium ion intermediate of the drug molecule accepts electron density from the N7 center of the guanine base. Therefore, the position as well as the stability of the LUMO (lowest unoccupied molecular orbital) of the aziridinium ion becomes more important [13]. It is important to note that, during the interaction of the drug molecule with the guanine (in DNA) the aziridinium ion opens up i.e. during mono-adduct formation, the $\angle\text{NCC}$ bond angle increases. However, the LUMO of the drug intermediate (i.e., with $\angle\text{NCC} = 60^\circ$) is localized away from the tricyclic ring. This clearly shows that the interaction of the drug intermediate (C atoms of the tricyclic ring in aziridinium ion) with the guanine (N7 atom) is not feasible. Therefore, our objective in this article is to examine how the position of the LUMO of the drug intermediate shifts with a variation in $\angle\text{NCC}$ bond angle in gas phase as well as in aqueous medium. We have chosen water as a solvent medium because most of our body fluid contains water. Apart from this, we have observed the variation of reactivity descriptors such as the chemical potential, hardness, and electrophilicity index, with the variation in $\angle\text{NCC}$ bond angle. Finally, the maximum hardness principle (MHP) [28] and minimum electrophilicity principle (MEP) [27] have been analyzed, using mustine an example.

2. Theoretical details of reactivity descriptors

Conceptual density functional theory defines the chemical potential μ as the first derivative of energy with respect to the number of electrons [25],

$$\mu = \left(\frac{\partial E}{\partial N} \right)_{v(\vec{r})} \quad (1)$$

and global hardness, (η) as [26]

$$\eta = \frac{1}{2} \left(\frac{\partial^2 E}{\partial N^2} \right)_{v(\vec{r})} = \frac{1}{2} \left(\frac{\partial \mu}{\partial N} \right)_{v(\vec{r})} \quad (2)$$

where E is the energy and N is the number of electrons of an electronic system at constant external potential, $v(\vec{r})$.

However, the finite difference approximation defines the above quantities in terms of ionization potential (IP) and electron affinity (EA) of the system [19].

$$\text{IP} = E_{N-1} - E_N \quad (3)$$

$$\text{EA} = E_N - E_{N+1} \quad (4)$$

where E_N , E_{N-1} and E_{N+1} are energies of N , $N-1$ and $N+1$ electron system.

In most numerical applications, chemical potential (μ) and chemical hardness (η) are calculated using finite difference approximation in terms of IP and EA and therefore, μ and η , given below, can be used as a working formula

$$\mu = \frac{-\text{IP} - \text{EA}}{2} \quad (5)$$

$$\eta = \frac{\text{IP} - \text{EA}}{2} \quad (6)$$

Recently, Parr and his coworkers proposed electrophilicity index as a measure of electrophilicity of a ligand (ω) as [29]

$$\omega = \frac{\mu^2}{2\eta} \quad (7)$$

It is a measure of the capacity of species to accept an arbitrary number of electrons.

3. Computational details

The structure of the drug intermediate was optimized using B3LYP/6-311++G (d,p) level of theory in gas phase. The frequency calculation was performed to confirm the minima. Thereafter, single point calculations were performed at various $\angle\text{NCC}$ bond angles using same level of theory. Initially, the $\angle\text{NCC}$ bond angle of the drug intermediate was increased by 1° from 60° to 70° and then a 10° increment up to 150° . The IP and EA were calculated from the three point finite difference approximation (Eqs. (3) and (4)). The global reactivity descriptors such as chemical potential, hardness and electrophilicity index were calculated from the Eqs. (5)–(7), respectively. All calculations were performed using Gaussian09 [30]. Similarly, the reactivity indices were computed in solvent phase using PCM (Polarizable Continuum Model) and water as a solvent [31]. In addition, to check the consistency of our results, we have performed single point calculations with augmented correlation consistent double zeta valence with p polarization function basis set (aug-cc-pVDZ) with B3LYP functional.

4. Results and discussion

4.1. Position of LUMO in the drug intermediate

The position of the LUMO of the aziridinium ion is very much important during the alkylation process and therefore, we have followed the position of the LUMO at various $\angle\text{NCC}$ bond angles. At first, we have varied the $\angle\text{NCC}$ bond angle from 60° to 70° , with an increment of 1° and thereafter, the bond angle was varied up to 150° , with an increment of 10° and observed the shape of the LUMO at each angle. The shape of the LUMO for $\angle\text{NCC}$ bond angles $60^\circ, 65^\circ, 70^\circ, 80^\circ, 90^\circ, 100^\circ, 110^\circ$ and 120° are presented in the Fig. 1. Other LUMO's are presented in Supporting information.

It was observed that at $\angle\text{NCC} = 60^\circ$, the LUMO is largely associated with the chloroethyl side chain, Fig. 1a. This position of LUMO cannot explain the alkylation reaction between the aziridinium ion intermediate and guanine base (in DNA). As the bond angle increases, the position of the LUMO starts shifting towards the tricyclic ring and at $\angle\text{NCC} = 65^\circ$, we have observed partial shifting of the LUMO to C5 position of the ring, Fig. 1b. On increasing the $\angle\text{NCC}$ bond angle further, it was observed that a large portion of the LUMO shifted towards the ring carbon and finally, there was a complete shifting of the LUMO at $\angle\text{NCC}$ bond angle more than 70° (Fig. 1c–h). Thus we have observed significant shifting of the LUMO towards the ring carbon with variation of $\angle\text{NCC}$ bond angle. This shifting in the position of the LUMO clearly indicates that, for the drug intermediate to interact with guanine, the tricyclic ring must open up. This would facilitate the ring carbon in the drug intermediate to accept electron density from the guanine base. More specifically, the aziridinium ion intermediate must undergo some structural changes in order to alkylate DNA. In addition, the values of the coefficients of the atomic orbitals of LUMO provided similar information. Similar results were observed with different basis set, B3LYP/aug-cc-pVDZ.

4.2. Variation of HOMO and LUMO energies

Now, we would like to throw some light on the HOMO and LUMO energies of the drug intermediate which can be approximated as the negative of IP and EA, respectively, by Koopmans' approximation. We would like to monitor the stability of the LUMO with variation in $\angle\text{NCC}$ bond angle. This would, in turn, facilitate

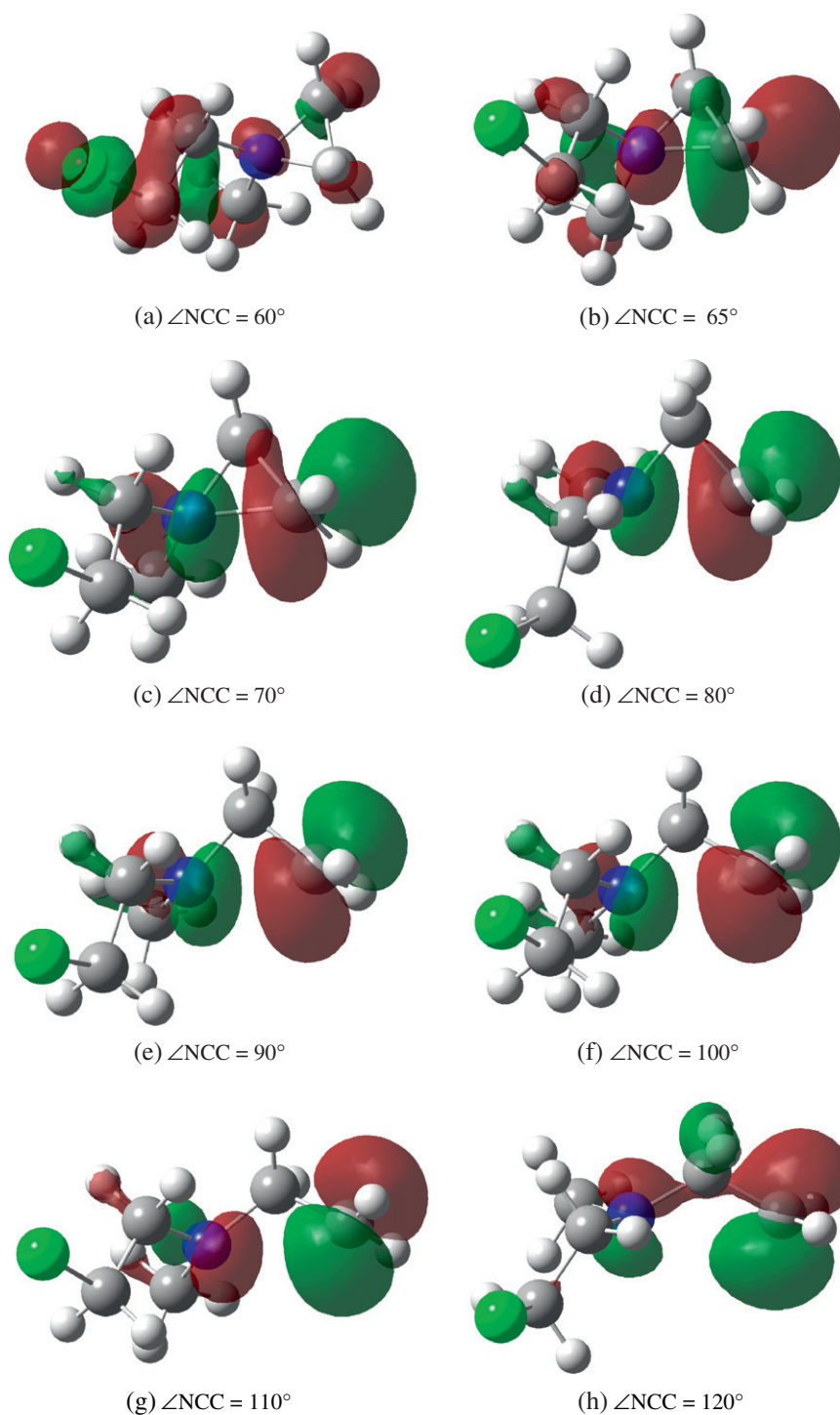


Fig. 1. Localization of LUMO with different NCC bond angle in aziridinium ring of the drug intermediate.

the acceptance of electron density from the guanine base. However, there are several limitations in the calculation of IP and EA using the Koopmans' approximation. In general, the ΔSCF methodology reliably yields IP and EA values compared to the Koopmans' theorem. The values of the HOMO and LUMO energy of the drug intermediate with different $\angle\text{NCC}$ bond angle (from 60° to 150°) in gas phase are presented in Tables 1 and 2 while for solvent medium in Tables 3 and 4. However, in Figs. 2 and 3, we have compared the variation in IP and EA, calculated from the two methods (Koopmans' approximation and ΔSCF method), with the variation in $\angle\text{NCC}$ bond angle in gas phase.

As we go on increasing the $\angle\text{NCC}$ bond angle from 60° to 120° , HOMO became unstable (more positive value of HOMO energy) while the LUMO became stable (Tables 1–4). For instance, HOMO energy (negative of IP) increases from -0.4402 at 60° to -0.4144 at 120° of bond angle (Table 1 and Fig. 2). On the other hand, LUMO energy (negative of EA), varies from -0.1628 at 60° to -0.3689 at 120° (Table 1 and Fig. 3). However, with further increase in $\angle\text{NCC}$ bond angle (from 130° to 150°), reverse trend was observed (Table 1; Figs. 3 and 4). Thus, cleavage of the C5–N3 bond (Fig. 5) (on increasing the $\angle\text{NCC}$ bond angle) results in more stabilization of the LUMO and facilitates the acceptance of electron density from

Table 1
Values of HOMO and LUMO energy, IP and EA (calculated by Δ SCF), chemical potential (μ), hardness (η) and electrophilicity (ω) of the drug intermediate with different values of NCC bond angle at B3LYP/6-311++G (d,p) level in gas phase.

NCC bond angle (in degrees)	ϵ_{HOMO}	ϵ_{LUMO}	IP $_{\Delta\text{SCF}}$	EA $_{\Delta\text{SCF}}$	μ	η	ω
60	-0.4402	-0.1628	0.5452	0.1134	-0.3293	0.2159	0.5023
70	-0.4367	-0.2094	0.5391	0.1342	-0.3367	0.2025	0.5598
80	-0.4336	-0.2765	0.5296	0.1961	-0.3629	0.1668	0.7896
90	-0.4307	-0.3220	0.5176	0.2423	-0.3800	0.1376	1.0490
100	-0.4277	-0.3517	0.5027	0.2745	-0.3886	0.1141	1.3233
110	-0.4237	-0.3715	0.4862	0.2971	-0.3916	0.0946	1.6218
120	-0.4144	-0.3689	0.4815	0.3037	-0.3926	0.0889	1.7337
130	-0.4219	-0.3574	0.4885	0.2890	-0.3887	0.0998	1.5149
140	-0.4246	-0.3457	0.4936	0.2744	-0.3840	0.1096	1.3459
150	-0.4250	-0.3326	0.4971	0.2589	-0.3780	0.1191	1.1994

Table 2
Values of HOMO and LUMO energy, IP and EA (calculated by Δ SCF), chemical potential (μ), hardness (η) and electrophilicity (ω) of the drug intermediate with different values of NCC bond angle at B3LYP/aug-cc-pVDZ level in gas phase.

NCC bond angle (in degrees)	ϵ_{HOMO}	ϵ_{LUMO}	IP $_{\Delta\text{SCF}}$	EA $_{\Delta\text{SCF}}$	μ	η	ω
60	-0.4400	-0.1623	0.5446	0.1135	-0.3290	0.2155	0.5024
70	-0.4366	-0.2081	0.5385	0.1338	-0.3361	0.2024	0.5583
80	-0.4336	-0.2749	0.5288	0.1952	-0.3620	0.1668	0.7858
90	-0.4307	-0.3204	0.5166	0.2414	-0.3790	0.1376	1.0440
100	-0.4276	-0.3501	0.5015	0.2736	-0.3876	0.1140	1.3180
110	-0.4232	-0.3699	0.4848	0.2962	-0.3905	0.0943	1.6176
120	-0.4133	-0.3674	0.4801	0.3026	-0.3913	0.0888	1.7253
130	-0.4210	-0.3557	0.4874	0.2877	-0.3876	0.0998	1.5044
140	-0.4242	-0.3440	0.4925	0.2730	-0.3828	0.1097	1.3354
150	-0.4249	-0.3307	0.4960	0.2574	-0.3767	0.1193	1.1893

Table 3
Values of HOMO and LUMO energy, IP and EA (calculated by Δ SCF), chemical potential (μ), hardness (η) and electrophilicity (ω) of the drug intermediate with different values of NCC bond angle at B3LYP/6-311++G (d,p) level in aqueous phase.

NCC bond angle (in degrees)	ϵ_{HOMO}	ϵ_{LUMO}	IP $_{\Delta\text{SCF}}$	EA $_{\Delta\text{SCF}}$	μ	η	ω
60	-0.3219	-0.0209	0.3320	0.0342	-0.1831	0.1489	0.2252
70	-0.3206	-0.0494	0.3302	0.0577	-0.1940	0.1363	0.2761
80	-0.3193	-0.1148	0.3211	0.1159	-0.2185	0.1026	0.4655
90	-0.3059	-0.1598	0.3025	0.1611	-0.2318	0.0707	0.7599
100	-0.2884	-0.1889	0.2810	0.1922	-0.2366	0.0444	1.2614
110	-0.2721	-0.2080	0.2616	0.2132	-0.2374	0.0242	2.3289
120	-0.2571	-0.2088	0.2536	0.2191	-0.2363	0.0172	3.2418
130	-0.2672	-0.1962	0.2626	0.2058	-0.2342	0.0284	1.9311
140	-0.2743	-0.1844	0.2699	0.1919	-0.2309	0.0390	1.3667
150	-0.2798	-0.1708	0.2758	0.1765	-0.2262	0.0496	1.0310

Table 4
Values of HOMO and LUMO energy, IP and EA (calculated by Δ SCF), chemical potential (μ), hardness (η) and electrophilicity (ω) of the drug intermediate with different values of NCC bond angle at B3LYP/aug-cc-pVDZ level in aqueous phase.

NCC bond angle (in degrees)	ϵ_{HOMO}	ϵ_{LUMO}	IP $_{\Delta\text{SCF}}$	EA $_{\Delta\text{SCF}}$	μ	η	ω
60	-0.3212	-0.0206	0.3316	0.0351	-0.1833	0.1482	0.2268
70	-0.3199	-0.0485	0.3297	0.0573	-0.1935	0.1362	0.2748
80	-0.3185	-0.1135	0.3199	0.1150	-0.2175	0.1024	0.4615
90	-0.3044	-0.1585	0.3010	0.1601	-0.2305	0.0704	0.7545
100	-0.2869	-0.1876	0.2794	0.1913	-0.2353	0.0440	1.2571
110	-0.2707	-0.2069	0.2599	0.2123	-0.2361	0.0238	2.3431
120	-0.2560	-0.2074	0.2521	0.2180	-0.2350	0.0171	3.2388
130	-0.2660	-0.1948	0.2611	0.2045	-0.2328	0.0283	1.912
140	-0.2731	-0.1829	0.2685	0.1905	-0.2295	0.0390	1.3495
150	-0.2785	-0.1693	0.2744	0.1750	-0.2247	0.0497	1.0168

N7 of guanine. Similar trend in the results were observed in aqueous phase and with a different basis set, B3LYP/aug-cc-pVDZ (Tables 2–4). Further, comparing the results of IP and EA by Koopmans' approximation and Δ SCF method showed similar trend.

4.3. Variation of the reactivity descriptors

The values of the global reactivity descriptors such as chemical potential, hardness and electrophilicity index with different \angle NCC bond angle in gas phase and aqueous phase are presented in Tables 1–4 and Figs. 4, 6–8.

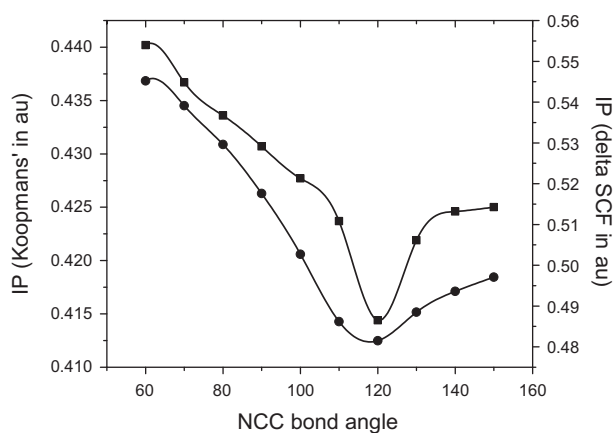


Fig. 2. Variation in IP values (square-Koopmans' approximation and circle- Δ SCF method) with the variation in the \angle NCC bond angle at B3LYP/6-311++G (d,p) level in gas phase.

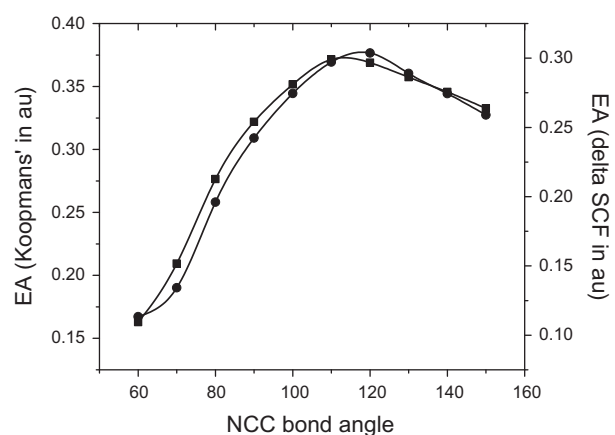


Fig. 3. Variation in EA values (square-Koopmans' approximation and circle- Δ SCF method) with the variation in the \angle NCC bond angle at B3LYP/6-311++G (d,p) level in gas phase.

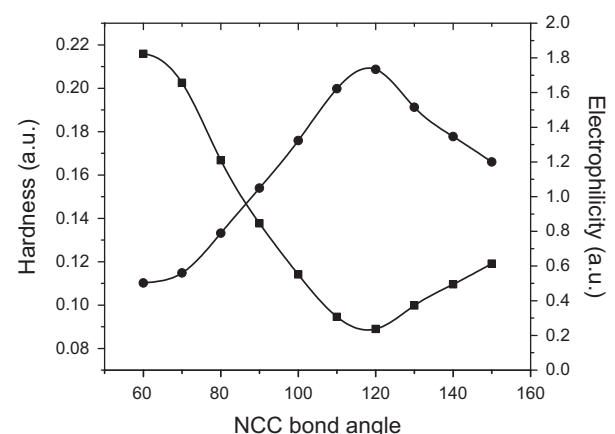


Fig. 4. Variation in hardness (square) and electrophilicity (circle) (both in au) for the drug intermediate with NCC bond angle at B3LYP/6-311++G (d,p) level in gas phase.

It was observed that the chemical potential and hardness passes through an extremum on increasing the \angle NCC bond angle, from 60° to 150° (Figs. 4, 6–8; Tables 1–4). The hardness values, for instance, has a minimum at 60°. Therefore, from the global point of view, these observations suggested that the stability of the drug

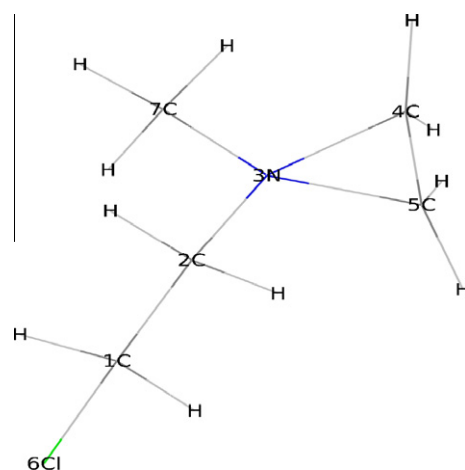


Fig. 5. Optimized geometry of the aziridinium ion intermediate of mustine drug molecule.

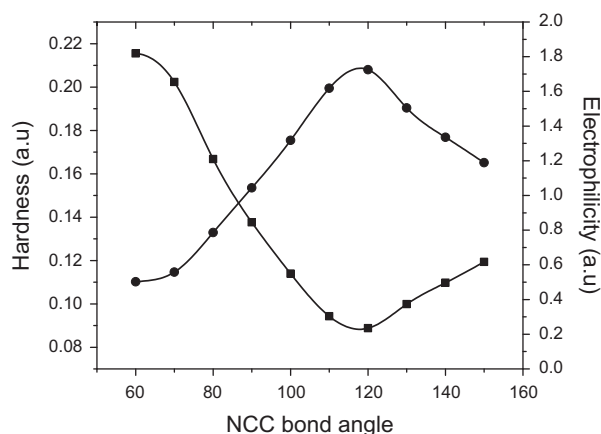


Fig. 6. Variation in hardness (square) and electrophilicity (circle) (both in au) for the drug intermediate with NCC bond angle at B3LYP/aug-cc-pVDZ level in gas phase.

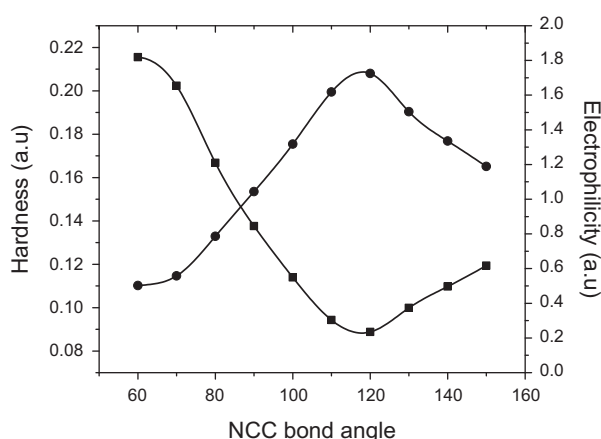


Fig. 7. Variation in hardness (square) and electrophilicity (circle) (both in au) for the drug intermediate with NCC bond angle at B3LYP/6-311++G (d,p) level in aqueous phase.

intermediate is least with the \angle NCC bond angle of around 120°. The values of the electrophilicity index also suggested that the electrophilicity of the drug intermediate has a maximum at around 120° (Figs. 4, 6–8; Tables 1–4). The hardness has a minimum while

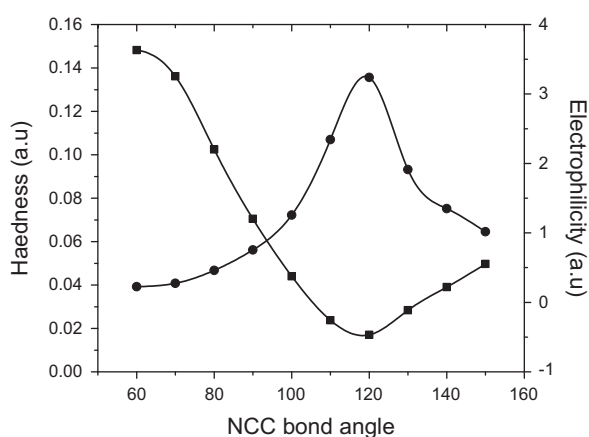


Fig. 8. Variation in Hardness (square) and Electrophilicity (circle) (both in au) for the drug intermediate with NCC bond angle at B3LYP/aug-cc-pVDZ level in aqueous phase.

the electrophilicity has a maximum around similar \angle NCC bond angle. Hence, the drug intermediate was found to be most prone to bind to DNA with \angle NCC bond angle around 120° . Similar trends were observed using different basis set, B3LYP/aug-cc-pVDZ and aqueous medium (Figs. 4, 6–8; Tables 1–4). It should be noted that the hardness and electrophilicity of the drug intermediate have a maxima and minima, respectively, at the equilibrium geometry. Earlier literature suggested that if hardness and chemical potential are maxima at any point along the internal coordinates, the corresponding electrophilicity is minimum at that point. Similarly, if chemical potential and hardness are minimum at any point, the corresponding electrophilicity is maximum [27]. Our studies also support the above findings and satisfy the minimum electrophilicity principle along with the maximum hardness principle.

5. Conclusion

In the present article, we have made an effort to examine how the position of LUMO in the aziridinium ion intermediate shifted with a variation in the \angle NCC bond angle of the tricyclic ring in gas phase as well as in aqueous phase using two different basis sets. As the \angle NCC bond angle increases, the position of the LUMO in the drug intermediate shifted towards the ring carbon which facilitates alkylation of DNA. Thus, it can be concluded that the drug intermediate must undergo some structural changes i.e., the tricyclic ring must open up before alkylating DNA. It was also observed that the global reactivity descriptors (chemical potential, hardness and electrophilicity) have an extremum as the \angle NCC bond angle is varied from 60° to 150° .

Acknowledgements

P.K.B acknowledges the financial support from Department of Science and Technology (SR/S1/PC-13/2009), New Delhi. R.K. acknowledges the University Grants Commission (UGC), New Delhi.

Appendix A. Supplementary material

Supplementary data associated with this article can be found, in the online version, at doi:10.1016/j.comptc.2011.03.017.

References

[1] F.A. Carey, R.J. Sundberg, *Advanced Organic Chemistry Part A: Structure and Mechanism*, Kluwer Academic/Plenum Publishers, New York, 2001.

[2] R. Kar, P.K. Bhattacharyya (communicated).
 [3] S. Pal, N. Vaval, R.K. Roy, *J. Phys. Chem.* 97 (1993) 4404.
 [4] (a) S.R. Rajsiki, R.M. Williams, *Chem. Rev.* 98 (1998) 2723;
 (b) P.D. Lawley, *BioEssays* 17 (1995) 561.
 [5] S. Neidle, M. Waring (Eds.), *Molecular Aspects of Anti-cancer Drug Action*, Verlag Chemie, Weinheim, 1994, p. 315.
 [6] C.P. Rhoads, *J. Am. Med. Assoc.* 131 (1946) 656.
 [7] (a) C.M. Haskel, *Cancer Treatment*, second ed., Saunders, Philadelphia, 1990;
 (b) A. Gilman, F.S. Philips, *Science* 103 (1946) 409;
 (c) K.W. Kohn, in: H. Tapiero, J. Robert, T.J. Lampidis (Eds.), *Anticancer Drugs*, INSERM, John Libbey Eurotext, London, Paris, 1989;
 (d) B.J. Sanderson, *A.J. Shield, Mutat. Res.* 355 (1996) 41.
 [8] D.M. Noll, T.M. Mason, P.S. Miller, *Chem. Rev.* 106 (2006) 277.
 [9] S.M. Rink, M.S. Solomon, M.J. Taylor, R.B. Sharanabasava, L.W. McLaughlin, P.B. Hopkins, *J. Am. Chem. Soc.* 115 (1993) 2551.
 [10] (a) P. Calabresi, R.E. Parks, in: A. Gilman, L.S. Goodman, T.W. Raol, F. Murad (Eds.), *The Pharmacological Basis of therapeutics*, Macmillan, New York, 1985;
 (b) A. Hamza, H. Borch, D.J. Vasilescu, *Biomol. St. Dyn.* 43 (1996) 915;
 (c) H. Borch, A. Hamza, D. Vasilescu, *J. Biomol. St. Dyn.* 43 (1996) 903.
 [11] B. Singer, *Nature* 264 (1976) 333.
 [12] D.T. Beranek, C.C. Weis, D.H. Swenson, *Carcinogenesis* 1 (1980) 595.
 [13] (a) A. Pullman, in: P.O.P. Ts'o, J.A.D. Paolo (Eds.), *Chemical Carcinogenesis Part A*, Marcel Dekker, New York, 1974;
 (b) B. Pullman, in: H. Weinstein, J.P. Green (Eds.), *Quantum Chemistry in Biomolecular Science*, The New York Academy of Science, New York, 1981;
 (c) G.B. Bauer, L.F. Provirk, *Nucleic Acid Res.* 25 (1997) 1211.
 [14] A. Pullman, B. Pullman, *Int. J. Quant. Chem.* 18 (1980) 245.
 [15] (a) P.D. Lawley, *Prog. Nucl. Acids Res. Mol. Biol.* 5 (1966) 89;
 (b) B. Singer, *Prog. Nucl. Acids Res. Mol. Biol.* 15 (1975) 219;
 (c) A. Masta, P.J. Gray, D.R. Philips, *Nucleic Acid Res.* 22 (1994) 3880.
 [16] (a) J. Hansson, R. Lewensohn, U. Ringborg, B. Nilsson, *Cancer Res.* 47 (1987) 2631;
 (b) S.M. Rink, M.S. Solomon, M.J. Taylor, S.B. Rajur, L.W. McLaughlin, P.B. Hopkins, *J. Am. Chem. Soc.* 115 (1993) 2551;
 (c) M.R. Osborne, D.E.V. Wilman, P.D. Lawley, *Chem. Res. Toxicol.* 8 (1995) 316.
 [17] C.C. Price, in: A.C. Sartorelli, D.J. Johns (Eds.), *Handbook of Experimental Pharmacology*, Spinger-Verlag, Berlin, vol. 38, No. 2, 1974
 [18] P.K. Shukla, P.C. Misra, S. Suhai, *Chem. Phys. Lett.* 449 (2007) 323.
 [19] R.G. Parr, W. Yang, *Density Functional Theory of Atoms and Molecules*, New York, Oxford University Press, 1989.
 [20] (a) T. Mineva, T. Heine, *J. Phys. Chem. A* 108 (2004) 11086;
 (b) G. Molteni, A. Ponti, *Chem. Eur. J.* 9 (2003) 2770;
 (c) R.K. Roy, *J. Phys. Chem. A* 107 (2003) 397;
 (d) P.K. Chattaraj, S. Sengupta, *J. Phys. Chem.* 100 (1996) 16126;
 (e) P.K. Chattaraj, A. Poddar, *J. Phys. Chem. A* 102 (1998) 9944.
 [21] (a) H.M.T. Nguyen, J. Peeters, M.T. Nguyen, A.K. Chandra, *J. Phys. Chem. A* 108 (2004) 484;
 (b) J. Melin, F. Aparicio, V. Subramanian, M. Galvan, P.K. Chattaraj, *J. Phys. Chem. A* 108 (2004) 2487;
 (c) S. Shetty, R. Kar, D.G. Kanhere, S. Pal, *J. Phys. Chem. A* 110 (2006) 252;
 (d) T. Mineva, *J. Mol. Struct: THEOCHEM* 762 (2006) 79;
 (e) R.K. Roy, A.K. Chandra, S. Pal, *J. Phys. Chem.* 98 (1994) 10447.
 [22] (a) P.K. Chattaraj, B. Maiti, *J. Phys. Chem. A* 105 (2001) 169;
 (b) G. Madjarova, A. Tadjer, T.P. Cholokova, A.A. Dobrev, T. Mineva, *J. Phys. Chem. A* 109 (2005) 387;
 (c) J.C. Santos, R. Contreras, E. Chamorro, P. Fuentealba, *J. Chem. Phys.* 116 (2002) 4311;
 (d) T. Mineva, N. Russo, E. Sicilia, M. Toscano, *Theor. Chem. Acc.* 101 (1999) 388;
 (e) M.L. Romero, F. Mendez, *J. Phys. Chem. A* 107 (2003) 5874;
 (f) F. Mendez, M.A. García-Garibay, *J. Org. Chem.* 64 (1999) 7061;
 (g) P.W. Ayers, R.G. Parr, *J. Am. Chem. Soc.* 122 (2000) 2010;
 (h) P.W. Ayers, R.G. Parr, *J. Am. Chem. Soc.* 123 (2001) 2007;
 (i) J.S.M. Anderson, J. Melin, P.W. Ayers, *J. Chem. Th. Comp.* 3 (2007) 375.
 [23] (a) P. Geerlings, F. De Proft, W. Langenaekar, *Chem. Rev.* 103 (2003) 1793;
 (b) P.K. Chattaraj, U. Sarkar, D.R. Roy, *Chem. Rev.* 106 (2006) 2065.
 [24] (a) H.S. De, S. Krishnamurty, S. Pal, *J. Phys. Chem. C* 113 (2009) 7101;
 (b) P.W. Ayers, R.G. Parr, *J. Chem. Phys.* 128 (2008) 184108;
 (c) P.W. Ayers, C. Morell, F. De Proft, P. Geerlings, *Chem.-A Eur. J.* 13 (2007) 8240;
 (d) J. Moens, P. Geerlings, G. Roos, *Chem.-A Eur. J.* 13 (2007) 8174;
 (e) P.W. Ayers, F. De Proft, A. Borgoo, P. Geerlings, *J. Chem. Phys.* 126 (2007) 224107;
 (f) N. Sablon, P.W. Ayers, F. De Proft, A. Borgoo, P. Geerlings, *J. Chem. Phys.* 126 (2007) 224108;
 (g) G. Roos, P. Geerlings, J. Messens, *J. Phys. Chem. B* 113 (2009) 13465;
 (h) R. Kar, K.R.S. Chandrakumar, S. Pal, *J. Phys. Chem. A* 111 (2007) 375;
 (i) R. Kar, S. Pal, *Theor. Chem. Acc.* 120 (2008) 375;
 (j) R. Kar, S. Pal, in: P.K. Chattaraj (Ed.), *Chemical Reactivity Theory: A Density Functional View*, CRC Press, Taylor & Francis, 2008, chapter 25, p. 363;
 (k) R. Kar, S. Pal, *Int. J. Quant. Chem.* 110 (2009) 1642.
 [25] (a) R.G. Parr, R.G. Pearson, *J. Am. Chem. Soc.* 105 (1983) 7512;
 (b) R.G. Pearson, *J. Am. Chem. Soc.* 107 (1985) 6801.
 [26] R.G. Parr, R.A. Donnelly, M. Levy, W.E. Palke, *J. Chem. Phys.* 68 (1978) 3801.

- [27] (a) E. Chamorro, P.K. Chattaraj, P. Fuentealba, *J. Phys. Chem. A* 107 (2003) 7068;
(b) R. Parthasarathi, M. Elango, V. Subramanian, P.K. Chattaraj, *Theor. Chem. Acc.* 113 (2005) 257.
- [28] R.G. Parr, P.K. Chattaraj, *J. Am. Chem. Soc.* 113 (1991) 1854.
- [29] R.G. Parr, L.V. Szentpaly, S. Liu, *J. Am. Chem. Soc.* 1999 (1922) 121.
- [30] M.J. Frisch, G.W. Trucks, H.B. Schlegel, G.E. Scuseria, M.A. Robb, J.R. Cheeseman, G. Scalmani, V. Barone, B. Mennucci, G.A. Petersson, H. Nakatsuji, M. Caricato, X. Li, H.P. Hratchian, A.F. Izmaylov, J. Bloino, G. Zheng, J.L. Sonnenberg, M. Hada, M. Ehara, K. Toyota, R. Fukuda, J. Hasegawa, M. Ishida, T. Nakajima, Y. Honda, O. Kitao, H. Nakai, T. Vreven, J. A. Montgomery, Jr., J.E. Peralta, F. Ogliaro, M. Bearpark, J.J. Heyd, E. Brothers, K.N. Kudin, V.N. Staroverov, T. Keith, R. Kobayashi, J. Normand, K. Raghavachari, A. Rendell, J.C. Burant, S.S. Iyengar, J. Tomasi, M. Cossi, N. Rega, J. M. Millam, M. Klene, J.E. Knox, J.B. Cross, V. Bakken, C. Adamo, J. Jaramillo, R. Gomperts, R.E. Stratmann, O. Yazyev, A. J. Austin, R. Cammi, C. Pomelli, J.W. Ochterski, R.L. Martin, K. Morokuma, V.G. Zakrzewski, G.A. Voth, P. Salvador, J.J. Dannenberg, S. Dapprich, A.D. Daniels, O. Farkas, J.B. Foresman, J.V. Ortiz, J. Cioslowski, D.J. Fox, Gaussian, Inc., Wallingf, Gaussian 09, Revision B.01
- [31] (a) S. Miertus, E. Scrocco, J. Tomasi, *J. Chem. Phys.* 55 (1981) 117;
(b) B. Mennucci, J. Tomasi, *J. Chem. Phys.* 106 (1997) 5151;
(c) R. Cammi, B. Mennucci, J. Tomasi, *J. Phys. Chem. A* 104 (2000) 5631.